

The high density ignition in FFHR helical reactor by neutral beam injection (NBI) heating

O. Mitarai⁽¹⁾, A. Sagara⁽²⁾, R. Sakamoto⁽²⁾, N. Yanagi⁽²⁾, T. Goto⁽²⁾, S. Imagawa⁽²⁾,
O. Kaneko⁽²⁾, and A. Komori⁽²⁾

1) Liberal Arts Education Center, Kumamoto Campus, Tokai University, 9-1-1 Toroku,
Kumamoto 862-8652, Japan

2) National Institute for Fusion Science, 322-6 Oroshi-cho, Toki, 509-5292, Japan

E-mail contact of main author: omitarai@ktmail.tokai-u.jp

Abstract

Actual heating systems have not been considered yet for reaching the ignition regime in FFHR helical reactor. Although NBI heating is a first candidate to access the low density and high temperature ignition regime, it is uncertain whether such system can be used to access the high density and low temperature ignition regime. In this work the foreseeable NBI energy of ~ 1.5 MeV is assumed and examined for reaching both ignition regimes in the FFHR. Together with the stabilizing technique of the thermal instability by the proportional-integral-derivative (PID) control algorithm based on the fusion power, we propose the new operation scenario to access the high-density ignition regime using neutral beam heating system with ~ 1.5 MeV energy. In this new scenario the density is kept at the low value less than $\sim 4 \times 10^{20} \text{ m}^{-3}$ to ensure the neutral beam penetration and the operating point passes near the saddle point on Plasma Operation Contour (POPCON) map. Above the density of $4 \times 10^{20} \text{ m}^{-3}$, high-density ignition is accessed by alpha heating after turning off NBI injection.

1. Introduction

FFHR has two ignition scenarios with the thermally stable low density and high temperature, and the thermally unstable high density and low temperature operations. The former operation scenario is also conceived in a tokamak reactor. Recent high plasma density up to $1.1 \times 10^{21} \text{ m}^{-3}$ achieved in large helical device (LHD) pellet injection experiments [1] stimulates exploring the high density and low temperature operation in FFHR. Although a high-density operation is advantageous to reduce the divertor heat flux via bremsstrahlung radiations and to ease the pellet penetration, its thermally unstable control and heating of the high-density plasma have been major issues. The first issue to stabilize the thermal instability has been solved by the PID control algorithm based on the fusion power in the FFHR2m helical reactor [2]. A very high energy NBI system with 5~6 MeV is required for full penetration into high-density plasmas, which might be impossible to construct.

In this paper we propose to use the NBI with the beam energy of ~ 1.5 MeV for both operation regimes in FFHR. In the thermally stable low density and high temperature operation, the density is relatively as low as $1.9 \times 10^{20} \text{ m}^{-3}$, then the NBI with ~ 1.5 MeV can be used. On the other hand, as the high density inhibits the neutral beam penetration, the new operation scenario is required to access the high-density ignition regime by NBI heating with ~ 1.5 MeV. In this new scenario the density is kept at the low value less than $\sim 4 \times 10^{20} \text{ m}^{-3}$ to ensure the NBI penetration and the operating point passes near the saddle point on POPCON. Above the density, high-density ignition is accessed by alpha heating after turning off NBI using the proposed PID control developed for the thermally unstable operational regime.

2. NBI penetration length and zero-dimensional equations

The NBI penetration e-folding length is calculated by

$$\lambda(n,T)[m] = \left[\int_{-1}^0 n(x) \sigma_{yan}(n,T) dx \right]^{-1} \quad (1)$$

where σ_{yan} is the cross section for the multi-step ionization for NBI [3]. Density profile is assumed as the square root of parabolic $\alpha_n=0.5$ for the thermally stable operation, and the peaked one with $\alpha_n=3$ for the thermally unstable operation, and the temperature profile is parabolic with $\alpha_T=1$. For $E_{NBI}=1.5$ MeV, the NBI penetration lengths for the peaked profile are $\lambda=2.43$ m and 1.13 m at the density of $n(0) \sim 2 \times 10^{20} \text{ m}^{-3}$ and $4 \times 10^{20} \text{ m}^{-3}$, respectively. For $E_{NBI}=1.0$ MeV, they are $\lambda=1.77$ m and 0.834 m at the density of $n(0) \sim 2 \times 10^{20} \text{ m}^{-3}$ and $4 \times 10^{20} \text{ m}^{-3}$, respectively. 1 MeV NBI is now planned for ITER project [4] and up to 2 MeV has been conceived. Tangential injection was employed in this study to decrease the initial shine-through power.

Prior to 1-dimensional analyses which would be performed in a numerical reactor project, simple 0-dimensional particle and power balance equations[5] are used for exploring new operation scenario. In this analysis, the global power balance equation is used together with the combined global particle balance equation for the electron density,

$$\frac{dn_e(0)}{dt} = \frac{1}{1-8f_o} \left[(1 + \alpha_n) S_{DT}(t) - \left\{ \frac{f_D + f_T}{\tau_p^*} + \frac{2f_\alpha}{\tau_\alpha^*} \right\} n_e(0) \right] \quad (2)$$

where f_o is the oxygen impurity fraction, α_n is the density profile factor, S_{DT} is the D-T fueling rate, f_D is the deuterium fraction to the electron density, f_T is the tritium fraction, f_α is the alpha ash fraction, τ_p^* is the effective D-T fuel particle confinement time, and τ_α^* is the effective helium ash confinement time. Feedback control of the fusion power is conducted by fueling rate $S_{DT}(t)$ given by

$$S_{DT}(t) = S_{DT0} \left\{ e_{DT}(P_f) + \frac{1}{T_{int}} \int_0^t e_{DT}(P_f) dt + T_d \frac{de_{DT}(P_f)}{dt} \right\} G_{fo}(t) \quad (3)$$

where $S_{DT0}=4 \times 10^{19} \text{ m}^{-3}/\text{s}$, T_{int} is the integral time, T_d is the derivative time, and the gain is $G_{fo}(t)=2$ to 50. Here, in the thermally stable regime, the error of the fusion power is given by

$$e_{DT}(P_f) = +(1 - P_f / P_{f0}) \quad (4)$$

where P_f is the measured fusion power and P_{f0} is the set value of the fusion power, and in the thermally unstable regime

$$e_{DT}(P_f) = -(1 - P_f / P_{f0}) \quad (5)$$

In this study we use the density control before the fusion power control phase,

$$e_{DT}(n) = +(1 - n_e(t) / n_{set}) \quad (6)$$

where n_{set} is the set value of the density. This is essentially for the thermally stable regime

In this analysis, the global power balance equation is used,

$$\frac{dW}{dt} = P_{EXT} - (P_L + P_B + P_S - P_\alpha) \quad (7)$$

where P_L is the total plasma conduction loss, P_B is the total bremsstrahlung loss, P_S is the total synchrotron radiation loss, P_α is the total alpha heating power, and alpha heating efficiency of $\eta_\alpha=0.98$. The external heating power P_{EXT} is feedback controlled in the stable operation regime and preprogrammed in the unstable operation regime. POPCON is the contour map of the heating power of $P_{HT} = (P_L + P_B + P_S - P_\alpha)$ plotted on the n-T plane. The helium ash confinement time ratio of $\tau_\alpha^*/\tau_E=4$ and the fuel particle confinement time ratio of $\tau_p^*/\tau_E=3$ have been used in the helium ash particle balance equation. The ISS95 confinement scaling [6] is used for the plasma conduction loss where γ_{ISS} and γ_{LHD} represent the confinement enhancement factors over the ISS95 and present LHD scalings, respectively.

FFHR2m is a commercial reactor ($R=15.7\text{m}$, $\bar{a}=2.5\text{m}$, and the volume averaged magnetic field $B_o=4.5\text{ T}$, and $P_f=3\text{ GW}$) and has a full blanket module around the torus[7]. For comparative and feasibility studies on ignition experiments in a reasonable size machine, the smaller experimental helical reactor (FFHR-C, $R=9\text{m}$, $\bar{a}=1.5\text{m}$, and $B_o=7\text{ T}$, and $P_f=1.1\text{ GW}$) with a partial blanket system has been studied where the blanket is only placed on the outboard side and the shield is placed in the inboard side due to no enough space.

Machine and ignition plasma parameters on the steady state value in the commercial reactor are listed in Table I.

TABLE I: PLASMA PARAMETERS AT THE STABLE AND UNSTABLE OPERATING POINTS IN FFHR2m2

		Steady state value		
		Stable operating point	Unstable operating point	
			Parabolic profile	Peaked profile
Major radius	R (m)	15.7		
Effective minor radius	\bar{a} (m)	2.5		
Polarity/Field period	ℓ/m	2/10		
Coil pitch parameter	γ	1.2		
Volume averaged magnetic field	B_o (T)	4.5		
Maximum magnetic field	$B_{o\max}$ (T)	12.1		
Coil magnetic energy	W_c (GJ)	160		
Blanket thickness	ΔB (m)	1.2		
Rotational transform	$\tau_{2/3}$	0.92		
Maximum NBI heating power	P_{EXT} (MW)	50		
Confinement factor over ISS95 scaling	γ_{ISS} (Minimum)	1.92 (1.85)		1.43 (1.43)
Confinement time	τ_E (s)	2.3	5.6	4.3
Helium ash fraction	f_α	0.041	0.04	0.045
Oxygen impurity fraction	f_o	0.0075		
Effective ion charge	Z_{eff}	1.50		
He ash confinement time ratio	τ_α^*/τ_E	4		
Fuel particle confinement time ratio	τ_p^*/τ_E	3		
Fusion alpha heating efficiency	η_α	0.9		
Operation density	$n_e(0)$ (10^{20} m^{-3})	1.8	4.5	8.4
Density limit factor over Sudo scaling	γ_{SUDO}	1.5	7.5	6.5
Density limit margin in the steady state	$[n(0)_{\text{lim}}/n(0)]$	1.24	1.75	1.41
Ion temperature	$T_i(0)$ (keV)	17.8	8.5	7.1
Ion to electron temperature ratio	T_i/T_e	1.0		
Density profile	α_n	0.5		3
Temperature profile	α_T	1.0		1
Beta value	$\langle\beta\rangle$ (%)	4.9	5.7	4.5
Plasma energy	W_p (GJ)	1.150	1.352	1.05
Fusion power	P_f (MW)	3000		
Neutron power	P_n (MW)	2400		
Alpha heating power	P_α (MW)	600x0.98=588		
Bremsstrahlung power	P_B (MW)	87	345	348
Synchrotron radiation power	P_S (MW)	4.2	0.9	0
Plasma conduction loss	P_L (MW)	497	240	240
Electric power output (thermal efficiency)	P_e (MW)	1000(33%)		
Neutron wall loading	Γ_n (MW/m ²)	1.48		
Heat flux to first wall	Γ_n (MW/m ²)	0.056	0.21	0.22
Heat flux to divertor for 0.1 m wet width (90 degree, $P_f/2\pi R*0.1*2$)	Γ_{div} (MW/m ²)	25.0	12.1	12.2

3. Thermally stable ignition regime accessed by NBI in FFHR2m2

During the access to the thermally stable low density and high temperature operation regime, NBI heating has not any problems due to the relatively low-density. Figure 1 shows the temporal evolution of plasma parameters of FFHR2m2 with $\gamma_{ISS}=1.92$ ($\gamma_{LHD}=1.2$). The external heating power of 40 MW is initially applied and then feedback controlled. The oscillation of the heating power appears but damps away, and then the external heating power is automatically switched off at 300 s, showing ignition. The central density in the steady state is $1.83 \times 10^{20} \text{ m}^{-3}$, which is smaller than the 1.5 times of the Sudo density limit [8], the ion temperature is 17.8 keV, and the average neutron wall loading is 1.5 MW/m^2 . Averaged beta value is 4.9 %, which is already achieved in LHD experiments. Beam penetration length during the NBI heating is larger than $\lambda/\bar{a} \sim 0.7$. Therefore, 1.5 MeV NBI is sufficient for heating.

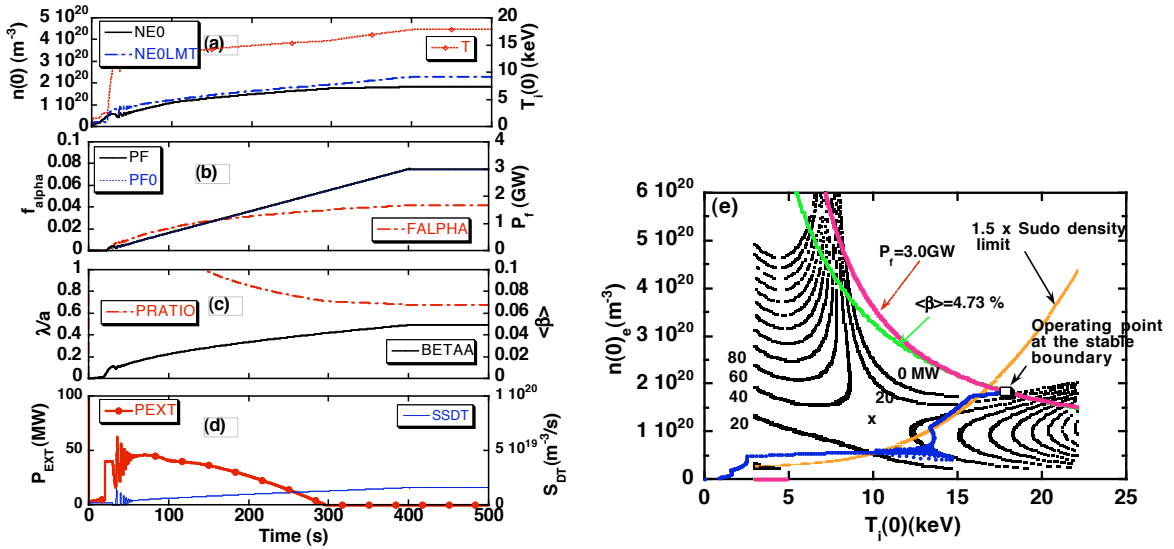


FIG. 1. Temporal evolution of plasma parameters in FFHR2m2 with the large pre-programming power of $P_{EXT-pre}=40 \text{ MW}$ and $\tau_{rise}=400 \text{ sec}$. (a) The peak ion temperature T , the peak density $NE0$, the density limit $NEOLMT$, (b) the alpha ash fraction $FALPHA$, the fusion power PF , its set value $PF0$, (c) the beam penetration ratio λ/\bar{a} , the plasma beta $BETAA$, (d) the external heating power $PEXT$ and the fueling rate, and (e) POPCON plot and operation path (blue line).

4. The high-density ignition regime accessed by NBI in FFHR2m2

In Fig. 2 is shown the temporal evolution of plasma parameters of FFHR2m2 with the confinement factor over ISS95 scaling of $\gamma_{ISS}=1.43$. To reduce the shine-through power, 1.5 MeV NBI is injected tangentially. The density linearly increases from $n(0)=2.0 \times 10^{20}$ to $3.0 \times 10^{20} \text{ m}^{-3}$ by the density control using Eq. (6). After the control is switched to the fusion power control at 35 s, the density is raised up due to alpha heating via fusion power control. The heating power is turned off at 38 s during the fusion power control phase. The NBI penetration ratio λ/\bar{a} is larger than 0.6 during heating phase as plotted in Fig. 2-(c). Required heating power P_{NBI} is 45 MW because the operation path goes near the saddle point on POPCON as shown in Fig.2-(e). Final operating point at the steady state is $n(0) \sim 9.3 \times 10^{20} \text{ m}^{-3}$ and the peak temperature is $T_i(0) \sim 6.8 \text{ keV}$, the volume averaged beta value is $\langle \beta \rangle \sim 4.7 \%$, the effective charge is $Z_{eff} \sim 1.53$, the average neutron wall loading is $\Gamma_n \sim 1.5 \text{ MW/m}^2$, the divertor heat load is $q_{div} \sim 9.4 \text{ MW/m}^2$ for the 10 cm width of the divertor plate perpendicular to

the magnetic field line.

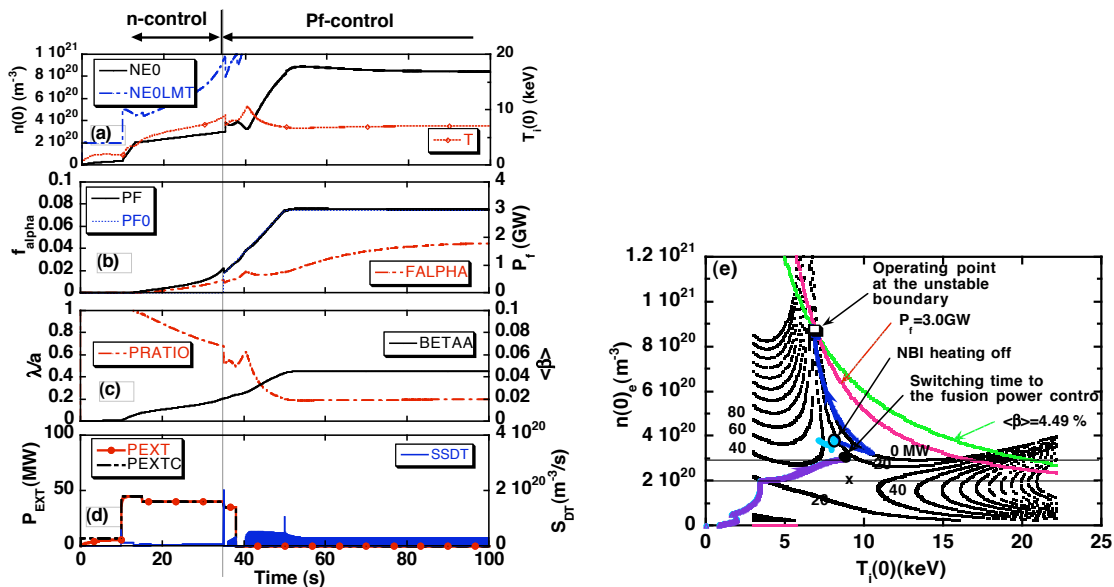


FIG. 2. Temporal evolution of plasma parameters in FFHR2m2 with the large pre-programming power of $P_{EXT-pre} = 45 \text{ MW}$ and $\tau_{rise} = 40 \text{ sec}$. (a)-(d) are the same as in Fig. 1, and (e) the solid circle on the operation path shows switching time from the density to fusion power control, and the open circle shows NBI turn off time.

Sensitivity analysis on the confinement factor has been conducted during the density control phase. After 30 s (which is 5 s before the switching time to the fusion power control), the confinement factor is artificially increased by a step manner from 1.43 to 1.6 as shown in Fig.3-(c). As seen in Fig.3-(b), the fusion power starts to increase at 30 s, and reaches 3 GW in a short time, and then terminates. As the height of the heating power contour line near the saddle point on POPCON as shown in Fig.3-(e) is lowered by the increment of the confinement factor, the operating point moves quickly to the high temperature side with the constant density. As the density is controlled by the feedback during the fusion power surge in the density control phase, the fusion power increases due to

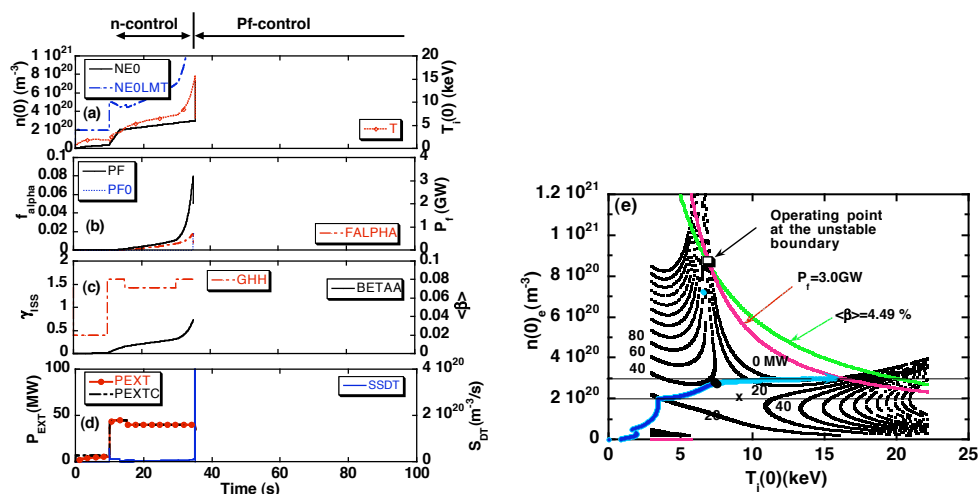


FIG. 3. Temporal evolution of plasma parameters when the confinement factor suddenly increased from 1.43 to 1.6 after 30 s in 15.7m reactor. (a)-(d) are the same as in Fig. 1 except for (c) with the confinement time factor, and (d) the solid circle shows the starting point of the thermal runaway.

the increase in the temperature. As this density control algorithm is based on a thermally stable control, its control algorithm is not suitable if it is used near the saddle point. However, as fueling is suddenly increased after the fusion power control is switched on at 35 s, the temperature goes down and fusion power quickly decreases. Most dangerous situation is avoided by this massive fueling. This is because the fueling takes place when the fusion power is larger than the set value of the fusion power ($P_f > P_{f0}$) in the successive fusion power control phase.

On the other hand, during 30 to 35 s, when the confinement factor is decreased by a step manner from 1.43 to 1.3, the fusion power decreases and then the discharge terminates. This is an automatic safe shutdown. This takes place when the height of the contour map of the heating power on POPCON increases due to the drop of the confinement factor. To proceed to the operating point, further heating power should be applied to overpass the contour map.

These sensitivity analyses show the fusion power control should be employed from the initial phase to avoid the dangerous situation. In Fig. 4, the density control is used until 12.8 s, and then fusion power control starts. To ensure the NBI penetration, the density is controlled to $2 \sim 3 \times 10^{20} \text{ m}^{-3}$ through the careful preprogramming of the fusion power. During the heating phase the penetration ratio is larger than 0.4.

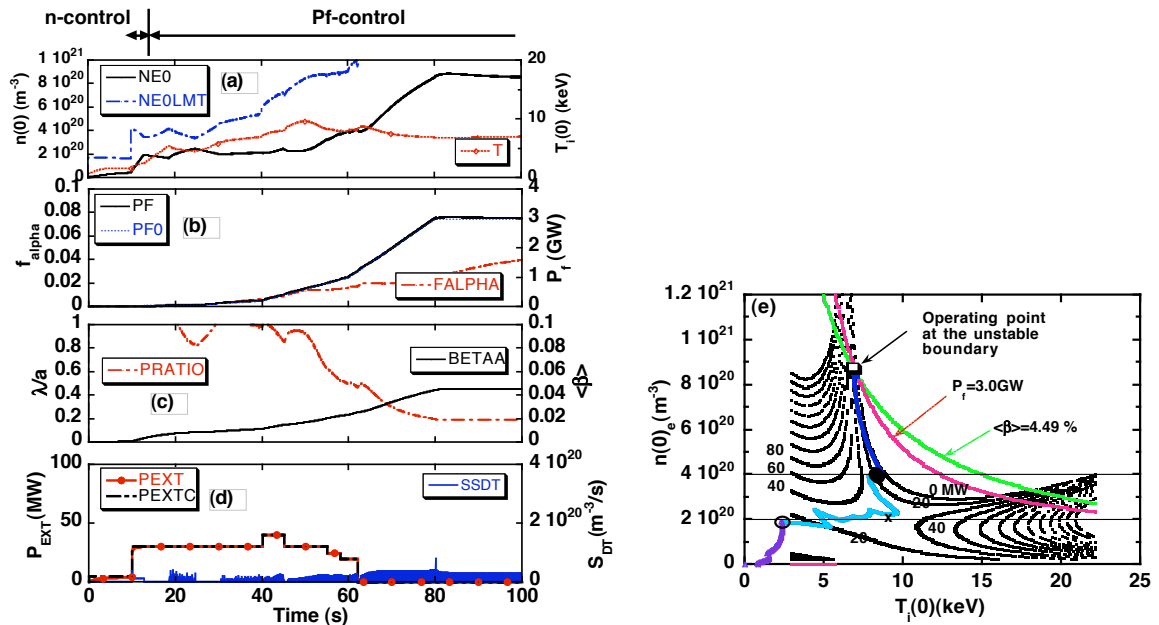


FIG. 4. Temporal evolution of plasma parameters when the unstable control algorithm is applied from 12.8 s. (a)-(d) are the same as in Fig. 1, and (e) POPCON where the solid circle shows the NBI turn off time with $\lambda/a=0.47$. The open circle shows the switching time to the fusion power control from the initial density control.

This control algorithm is robust to the confinement factor disturbance as shown in Fig. 5. When the confinement factor is increased during 40 to 60 s (between solid circles in Fig. 5-(e)), only the density is increased but the fusion power is well controlled. Even near the saddle point, this control algorithm works satisfactorily. Unstable density control algorithm has been used in the initial phase before 12.8 s until the open circle in Fig. 4-(e), which is necessary to go toward the high-density operation regime. However, as it is far from the saddle point, it might be safe when the parameters change.

Of course, when the confinement factor is decreased by a step manner from 1.43 to 1.3, the fusion power decreases and then the discharge terminates as with the density control. Therefore it leads to the safe shutdown of a discharge.

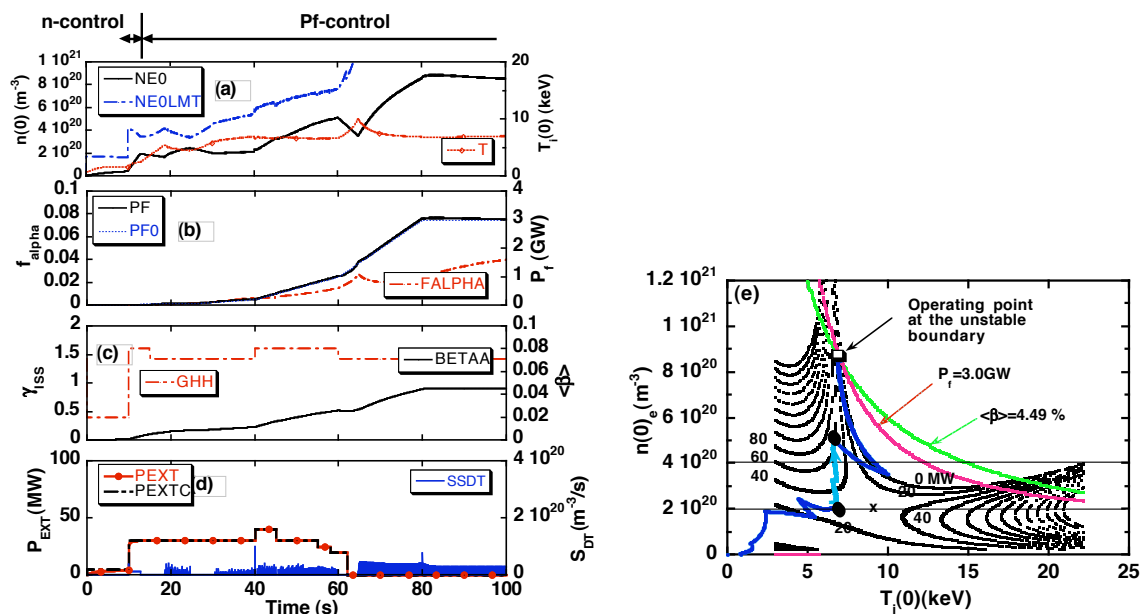


FIG. 5. Temporal evolution of plasma parameters when the unstable control algorithm is applied from 12.8 s and confinement factor suddenly increased during 40 to 60 s. (a)-(d) are the same as in Fig. 3, and (e) POPCON where the confinement factor increases between two solid circles.

5. The high-density ignition regime accessed by NBI in FFHR-C

If ignition experiments could be done in the compacter machine, it is quit helpful to develop the helical reactor. Therefore, we have surveyed the possibility of the smaller ignition machine around the major radius of 8~9 m, which is 2.2~2.5 times larger than the present LHD. As wide ignition regime is not obtained in the 8 m machine, we surveyed 9m machine in this work.

In the thermally stable ignition regime in the ignition experimental FFHR-C reactor ($R=9\text{m}$, $\bar{a}=1.5\text{m}$, and the volume averaged magnetic field $B_o=7\text{ T}$, and $P_f=1.1\text{ GW}$) with the parameters of $\alpha_n=1$, $\alpha_r=1$, $\gamma_{ISS}=1.8$ ($\gamma_{LHD}=1.125$), $\tau_\alpha^*/\tau_E=4$, $\tau_p^*/\tau_E=3$, and $\eta_\alpha=0.98$, steady state parameters are $n(0)\sim 3.56\times 10^{20}\text{ m}^{-3}$, $T_i(0)\sim 13.5\text{ keV}$, $\langle\beta\rangle\sim 2.5\%$, $Z_{eff}\sim 1.49$, $\Gamma_n\sim 1.5\text{ MW/m}^2$, and $q_{div}\sim 15\text{ MW/m}^2$ for the 10 cm width of the divertor plate perpendicular to the magnetic field line. For 1 MeV energy with tangential injection, as the density is lower than this value during the heating phase, the NBI penetration ratio is $\lambda/\bar{a}>0.5$ in the density range of $n(0)<3.5\times 10^{20}\text{ m}^{-3}$. The NBI heating power is $\sim 40\text{ MW}$. When the volume averaged magnetic field is smaller than $B_o=7\text{ T}$, ignition regime disappears. Therefore, if the high magnetic field helical coils are developed, the smaller ignition machine could be conceived. However, as the shield thickness is as thin as $\sim 35\text{ cm}$ in the inboard side, nuclear heating of the helical coils might be one of problems.

In Fig. 6 are shown the temporal evolution of the plasma parameters of a high-density operation and POPCON in FFHR-C. In this high-density operation, the density control is not safe as in FFHR2m2, and then the fusion power control was employed from the initial phase. For parameters of $\gamma_{ISS}=1.4$, $\alpha_n=3$, and $\alpha_r=1$, the final operating point at the steady state is $n(0)\sim 9.2\times 10^{20}\text{ m}^{-3}$, $T_i(0)\sim 7.9\text{ keV}$, $\langle\beta\rangle\sim 2.3\%$, $Z_{eff}\sim 1.49$, $\Gamma_n\sim 1.5\text{ MW/m}^2$, and $q_{div}\sim 11\text{ MW/m}^2$. During NBI heating phase with 1 MeV energy, the penetration ratio is larger than 0.4. Alpha heating helps to approach ignition after turning off NBI.

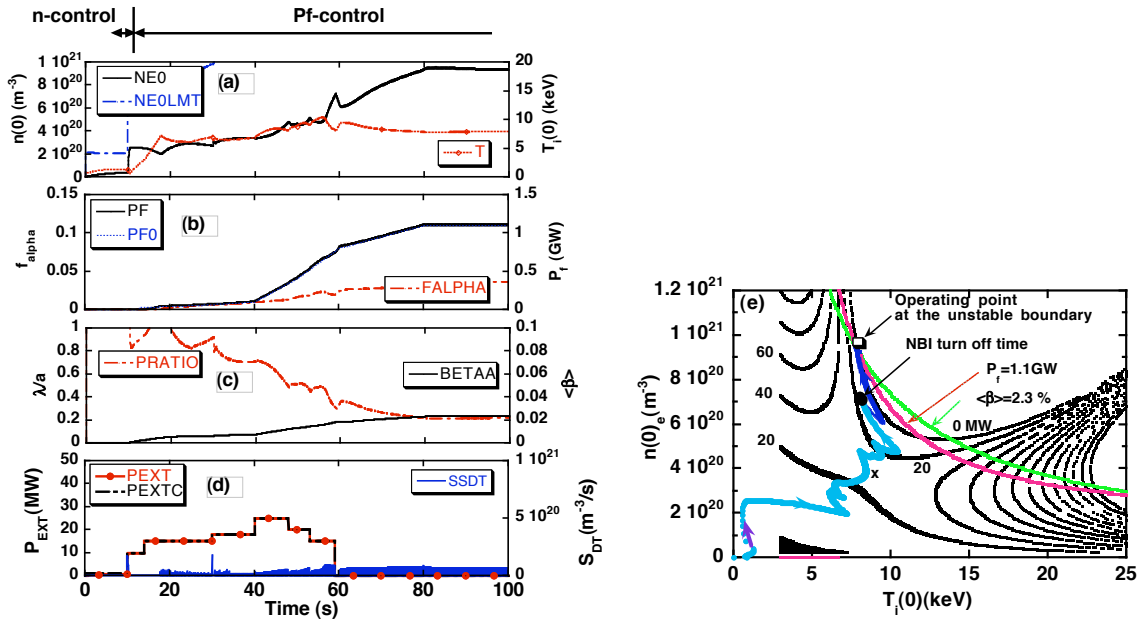


Fig 6. The temporal evolution of the high-density ignition using tangentially injected NBI with 1 MeV energy in FFHR-C. (a)-(d) are the same in Fig. 1.

6. Discussions and summary

We have studied how to use NBI heating in FFHR helical reactors. From a safe operating point view, the density control should be avoided especially near the saddle point on POPCON except for the only initial phase far from the saddle point. The fusion power for stabilizing the thermal instability can be carefully preprogrammed to have a low density for NBI penetration. After over passing the saddle point on POPCON, NBI heating power can be switched off. In this paper we demonstrated the effectiveness of the NBI heating even in the high-density operation as well as in the low density and high temperature operation in FFHR2m2 and FFHR-C.

As the NBI energy less than 1.5 MeV would also bring high-density ignition in the FFHR fusion ignition experimental and commercial reactor, the near term NBI technology [4] could be utilized for proposed helical reactors.

References

- [1] SAKAMOTO, R., et al., Nucl. Fusion, **49** (2009) 1.
- [2] MITARAI, O., SAGARA, et al., Plasma and Fusion Research, Rapid Communication, Vol.2 (2007) 021-1-3, and Fusion Science and Technology **56** (2009) 1495.
- [3] YANEV, R. K., et al., Nucl. Fusion, **29** (1989) 2125.
- [4] INOUE, T., et al., Fusion Engineering and Design, **81** (2006) 1291.
- [5] MITARAI, O., ODA, A., SAGARA, A., YAMAZAKI, K., and MOTOJIMA, O., Fusion Engineering and Design **70** (2004) 247
- [6] STROH, U., MURAKAMI, M., DORY, R. A., YAMADA, H., OKAMURA, S., SANO, F., and OBIKI, T., Nucl. Fusion **36**, (1996) 1063
- [7] SAGARA A., IMAGAWA, S., MITARAI, O., DOLAN, T., TANAKA, T., KUBOTA, Y. et al., Nucl. Fusion **45** (2005) 258. SAGARA A., MITARAI, O., TANAKA, T. et al., Fusion Engineering and Design **83** (2008) 1690–1695
- [8] SUDO, S., TAKEIRI, Y., ZUSHI, H., SANO, F., ITOH, K., KONDO, K., and IYOSHI, A., Nucl. Fusion, **30** (1990) 11